Reversal of the amplitude difference of kHz QPOs in six atoll sources

G. Török

Institute of Physics, Faculty of Philosophy and Science, Silesian University in Opava, Bezručovo nám. 13, 74601 Opava, Czech Republic
e-mail: terek@volny.cz

ABSTRACT

Context. Several models have been proposed to explain the twin kilohertz quasi-periodic oscillations (kHz QPOs) detected in neutron-star low-mass X-ray binaries; but when confronting theory with observations, not much attention has been paid so far to the relation between their amplitudes.

Aims. For six neutron-star atoll sources (namely 4U 1608-52, 4U 1636-53, 4U 0614+09, 4U 1728-34, 4U 1820-30, and 4U 1735-44), we investigate the relationship between the observed fractional rms amplitudes of the twin kHz QPOs. We discuss whether this relationship displays features that could have a physical meaning in terms of the proposed QPO models.

Methods. We consider the difference in rms amplitude between the upper and lower kHz QPOs as a function of the frequency ratio $R = \nu_U/\nu_L$. We compared two data sets. Set I is a collection taken from published data. Set II has values for the rms amplitudes obtained by automatic fitting of all RXTE-PCA observations available up to the end of 2004, corresponding to continuous segments of observation.

Results. For each of the six sources, we find that there is a point in the R domain around which the amplitudes of the two twin kilohertz QPOs are the same. We find such a point located inside a narrow interval $R = 1.5 \pm 3\%$. Further investigation is needed in the case of 4U 1820-30 and 4U 1735-44 to explore this finding, since we have not determined this point in Set II. There is evidence of a similar point close to $R = 1.33$ or $R = 1.25$ in the four sources 4U 1820-30, 4U 1735-44, 4U 1608-52, and 4U 1636-53. We suggest that some of these special points may correspond to the documented clustering of the twin kHz QPO frequency ratios.

Conclusions. For the sources studied, the rms amplitudes of the two twin peaks become equal when the frequencies of the oscillations pass through a certain ratio R, which is roughly the same for each of the sources. In terms of the orbital QPO models (of both the hot-spot and disc-oscillation types), with some assumptions concerning the QPO modulation mechanism, this finding implies the existence of a specific orbit at a particular common value of the dimensionless radius, at which the oscillations corresponding to the two twin peaks come into balance. In a more general context, the amplitude difference behaviour suggests a possible energy interchange between the upper and lower QPO modes.

Key words. X-rays: binaries – stars: neutron – accretion, accretion disks

1. Introduction

A number of black-hole and neutron-star sources in low-mass X-ray binaries (LMXBs) show quasi-periodic oscillations (QPOs) in their observed X-ray fluxes, i.e., narrow features (peaks) in their power density spectra (hereafter PDS). The frequencies of these QPOs range from $\sim 10^{-2}$ Hz to $\sim 10^3$ Hz. Here we restrict our attention to the so-called kHz (or high-frequency; HF) QPOs, which have frequencies in the range 200–1300 Hz, i.e., of the same order as the frequencies of orbital motion close to the compact object (see van der Klis 2006, for a review).

In black-hole systems HF QPO peaks are typically detected at constant frequencies characteristic of a given source. When two or more HF QPO frequencies are detected, they usually come in small-number ratios, typically in a 3:2 ratio (Abramowicz & Kluźniak 2001; McClintock & Remillard 2003). For neutron-star sources, on the other hand, kHz QPOs often arise as two simultaneously observed[1] peaks with

---

[1] The term "simultaneously observed" is here applied to continuous observations (or their subsegments) displaying both modes. The integration time needed for these detections ranges from a few seconds to a few dozen minutes.

frequencies that change over time. This paper focuses on these kHz PDS features, referred to as twin kHz QPOs.

From here on, we adopt the convention of calling the two peaks forming twin kHz QPOs the *lower and upper QPO* and denote their frequencies as $\nu_L < \nu_U$. The twin kHz QPOs span a wide frequency range and follow a nearly linear $\nu_U - \nu_L$ relation for each source (Belloni et al. 2005; Abramowicz et al. 2005b; Bursa 2006).

In this paper we use the twin kHz QPO data obtained with the Proportional Counting Array (PCA; Jahoda et al. 1986) on board the Rossi X-ray Timing Explorer (RXTE; Bradt et al. 1993).

1.1. Orbital models of kHz QPOs and frequency ratio

Several models have been proposed to explain kHz QPOs, and most of them involve orbital motion in the inner regions of the accretion disc (see van der Klis 2006; Lamb & Boutloukos 2007, for a recent review).

Among others, two frequently discussed models are based on strong-gravity properties. Stella & Vietri (1999) introduced the "relativistic precession model" (which we will refer to as the *RP model*) in which the QPOs are associated with the

motion of blobs of matter in the inner parts of the accretion disc. The upper and lower QPO frequencies ν_U, ν_L are identified with the Keplerian frequency and the relativistic periastron precession frequency, respectively. Slightly after this, Kluźniak & Abramowicz (2001) suggested a model in which the twin kHz QPOs arise from non-linear resonance between two modes of *accretion disc oscillation*. We will refer to this as the *resonance model*. In the basic version of the resonance model, the upper and lower QPO frequencies, when in a resonant ratio, coincide with the resonant frequencies given by specific combinations of epicyclic frequencies of geodesic test particle orbital motion (see Abramowicz & Kluźniak 2001; Abramowicz et al. 2003; Rebusco 2004; Horák & Karas 2006; Abramowicz et al. 2006; Fogelström et al. 2008).

Frequencies of geodesic motion at a given orbit, scale inversely with the mass M of the central compact object when the dimensionless forms of the neutron star angular momentum j and quadrupole moment q are held fixed. Therefore, within the framework of the above models, if the absolute differences between the squares of angular momenta are small among the sources being considered, the ratio $R = \nu_U/\nu_L$ between the twin kHz QPO frequencies represents a rough measure of the radial position of the QPO excitation, which is independent of the mass of the neutron star (Török et al. 2008). The frequency ratio R also has genuine importance for the resonance model.

1.2. Strength of the signal

Because of the expected links to the orbital motion, most discussions of neutron star twin kHz QPOs have for a long time been concentrated mainly on the frequencies ν_L, ν_U, and on their relations and evolution.

The other QPO properties, namely the *quality factor Q* and *fractional root-mean-squared (rms) amplitude r* have also been studied, but have not attracted such wide attention. We recall that the quality factor Q characterises the coherence time of a QPO, being defined as the QPO centroid frequency over the full-width of the peak at its half-maximum, while the fractional root-mean-squared amplitude r represents a measure of the signal strength, which is proportional to the square root of the peak power contribution to the PDS. In the past few years, both the quality factor and the rms amplitude have been studied systematically for several sources, and possible consequences for various QPO models have been outlined (see, e.g., Méndez 2006; Barret et al. 2006, for further information and references).

However, most attention has been focussed on the quality factor and the rms amplitude as separate functions of frequency. Little attention has been paid to the *mutual relations* between the (correlated) QPO amplitudes.

In the present work we study the difference in strength between the twin kHz QPOs, $\Delta r = r_L - r_U$, defined as the difference between the fractional rms amplitudes of the lower and upper kHz QPOs (r_L, r_U).

2. Data analysis

Here we focus on six well-studied atoll sources (namely 4U 1608–52, 4U 1636–53, 4U 0614+09, 4U 1728–34, 4U 1820–30, and 4U 1735–44) spanning a wide range of frequencies.

2.1. Published data (Set I)

We benefit from existing studies and use published results on rms amplitude correlations from the large collection made by Méndez (2006). We refer to this data as *Set I*. The main references to the original papers are as follows: 4U 1608-52 (Méndez et al. 2001), 4U 1636-53 (Barret et al. 2005a), 4U 0614+09 (van Straaten et al. 2002), 4U 1728-34 (Méndez et al. 2001), 4U 1820-30 (Barret et al. 2006), 4U 1735-44 (Barret et al. 2006). Although obtained in different studies (using different approaches), the data are comparable since they are measured over the whole RXTE-PCA energy band (2−60 keV).

The data of Set I do not always correspond directly to simultaneous twin kHz QPO measurements. Moreover, the range where the properties of either one of the QPO frequencies is well-investigated often extends far from the region of joint coverage, and then the identification of a particular significantly-detected peak as belonging to the upper or lower group comes from an extensive investigation of its properties (especially its quality factor) and also its correlations with the low-frequency QPOs (see Méndez et al. 2001; Olive et al. 2003; Barret et al. 2005a,b, 2006; Belloni et al. 2007; van der Klis 2006). It is relevant in this context that both QPOs become weak broad features when their frequencies are lower than ~500 Hz (see Olive et al. 2003).

For the purposes of this paper, we interpolate the amplitude data of Set I for each source using the best fits for both amplitudes made in terms of a sum of three exponentials

$$r_i = \sum_{j=1}^{3}\left[\exp\left(P_{i,j}^{(1)} + \nu_i P_{i,j}^{(2)}\right) + P_{i,j}^{(3)}\right], \quad i \in \{U, L\}, \tag{1}$$

with the $P_{i,j}^{(k)}$ being free parameters.

As noticed in several studies, the frequency correlations in the six sources considered in this paper are well-fitted by linear relations (Abramowicz et al. 2005a; Belloni et al. 2005; Bursa 2006; Zhang et al. 2006). *We use this property to connect both amplitude-frequency relations (1), with the assumption that the frequency correlations are linear in the range above ν_L = 500 Hz, and follow the relations found in Abramowicz et al. (2005a,b).* These relations were determined from the well-investigated twin QPO data above ν_L = 500 Hz, i.e., below $R \simeq 1.7$. The highest frequency ratio detections in the atoll sources being considered are around $R \sim 2.5-3$[2]. However, the detections above $R \sim 2$ are rare and an extension to the related range $\nu_L \sim 200-400$ Hz is subject to errors in determining the above relations.

2.2. Data processed in a uniform way (Set II)

Following Barret et al. (2005a, 2006), we use all public archival RXTE-PCA data available up to the end of 2004 (for the full energy band from 2−60 keV) for the six atoll sources that we are considering. Segments of the temporally continuous collection of data from a single pointing are processed using a shift-add procedure. For each segment, a set of 8-s leahy normalized PDS is produced, and an averaged PDS is then calculated for each set. The averaged PDS is searched for QPOs using a scanning technique that looks for peak excess (assumed to have a Lorentzian

---

[2] See Zhang et al. (2006) who study frequency correlations in a large group of sources using for the atoll sources the data from works of Belloni et al. (2002, 2005), Psaltis et al. (1999a,b), van der Klis (2000, 2006), Méndez et al. (1998a,b,c), Méndez & van der Klis (1999), van Straaten et al. (2000, 2002, 2003), Di Salvo et al. (2003), Jonker et al. (2002), Markwardt et al. (1999), Migliari et al. (2003).
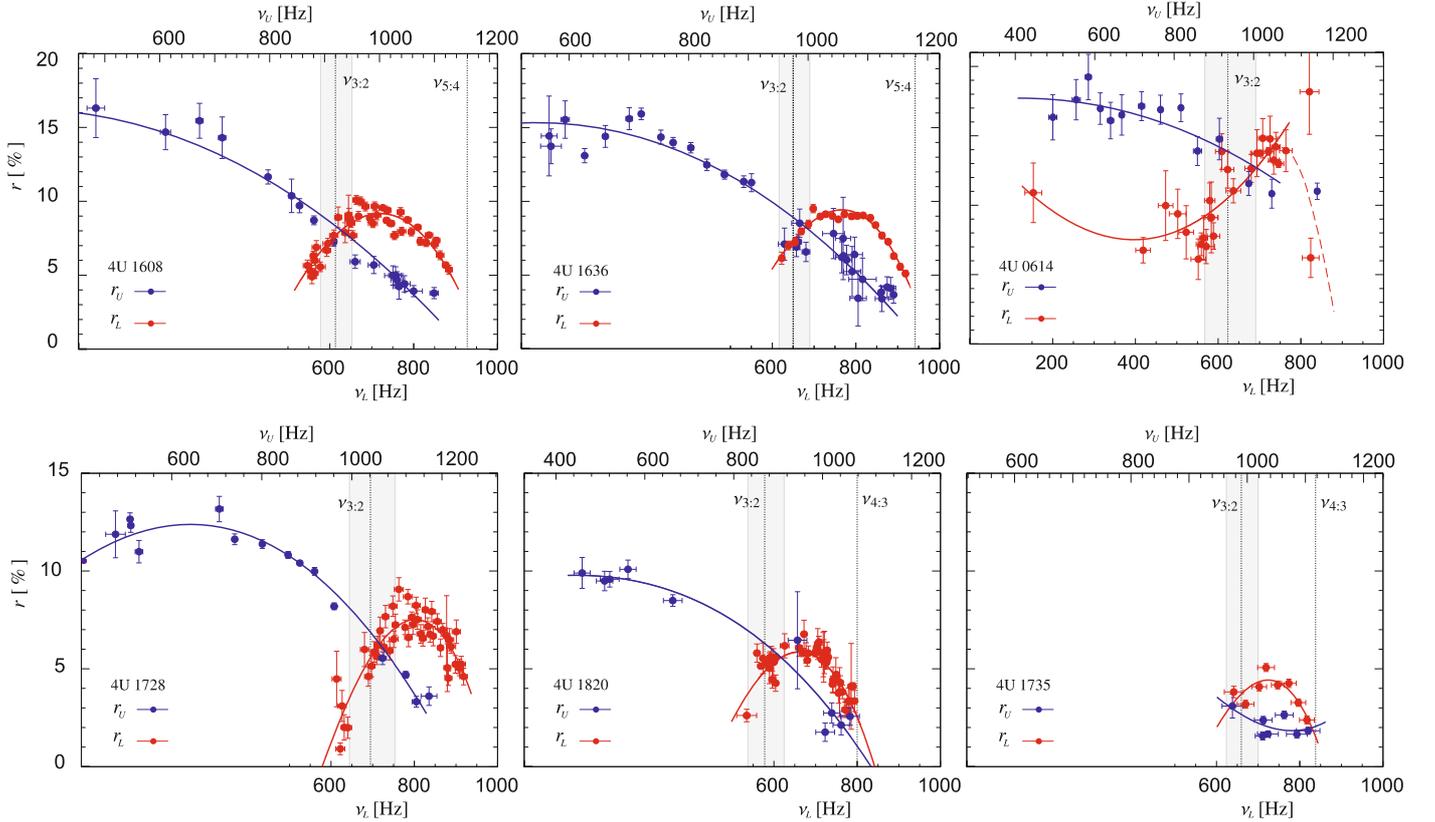
Fig. 1. Amplitudes of the lower and upper oscillations plotted against the two QPO frequencies (published data). Above $\nu_L \sim 500$ Hz (i.e., below $R \gtrsim 1.7$), the frequency correlations are approximated well by the linear relations that we use. The shadow indicates the frequency range corresponding to $R = 1.5 \pm 3\%$. For the lower QPO in 4U 0614+09 the high-frequency part contains two datapoints that do not indicate a clear trend.

profile) above the Poisson counting noise level (see Boirin et al. 2000). To minimize the effects of long-term frequency drift, the QPO frequencies are estimated on the shortest statistically permitted timescales, applying a recursive search algorithm seeking over the set of 8-s PDS. If there are two QPO peaks present in the segment-averaged PDS, the peak with the highest *significance S* (defined as the integral of the Lorentzian fitting of the peak divided by its error) is considered for further tracking. The tracked QPO is searched for within a window with a width not greater than 20% of the QPO frequency. The present frequency-ratio detections in the sources being considered are above $R = 1.2$. Because the relative frequency change within a single observation is small, the algorithm cannot switch between the two peaks within the tracking. After the tracking, the segment splits into several averaged subsegments (each of them corresponding to about 50−500 s) to which the shift-add is applied. The PDS obtained is then searched for the final QPOs. For later analysis, we retain the resulting peaks detected above the threshold $S \geq 2.5\sigma$. We refer to these data, representing a coherent set processed in a uniform way, as Set II.

3. Results

It can be seen from Fig. 1 that the rms amplitudes of the two peaks are comparable over a frequency range that is rather narrow with respect to the total frequency range spanned by the six sources. Moreover, for all of the six sources, the rms amplitudes are comparable in a range around the frequency where the 3:2 ratio occurs. We mark this frequency and those for other relevant ratios in Fig. 1.

Consideration of individual frequency correlations implies that lower and upper QPO datapoints overlaps in Fig. 1 do fall mostly within the range $R \sim 1.2–1.7$. In Fig. 2 we show the behaviour of the amplitude difference Δr in this range, as inferred from the interpolated curves in Fig. 1. In the same figure we also plot values of Δr from Set II. We detected only three significant datapoints outside this range in Set II. Each of these three datapoints falls into the range $R \in [2.2, 2.7]$ and corresponds to negative values of Δr.

3.1. Roots of Δr

The values of Δr at the intersection with the R axis are shown in Table 1. We refer to the intersections as "roots R_1, R_2", corresponding to the higher and lower frequency ratios.

In the four sources (4U 1608-52, 4U 1636-53, 4U 0614+09, 4U 1728-34) where we detected enough datapoints in Set II between $R = 1.4–1.6$, the values of Δr are well-approximated by linear functions of R in that range. We then fit these datapoints by straight lines (see Table 1 for the corresponding χ^2). For 4U 1636-53 and 4U 1608-52, which display in the Set II data a clear increase in amplitude difference between $R = 1.2–1.4$, we join the straight-line fit to an increasing exponential fit. All of the resulting curves for Set II are included in Fig. 2.

For the four sources 4U 1608-52, 4U 1636-53, 4U 0614+09, and 4U 1728-34, the roots R_1 for the Set II data given in Table 1 are determined from the fits described above. In principle, the fits can enable us also to determine the roots R_2 from the Set II data for 4U 1636-53 and 4U 1608-52. These are close to $R \sim 1.25$ but are difficult to quantify precisely. Clearly, as can be seen from
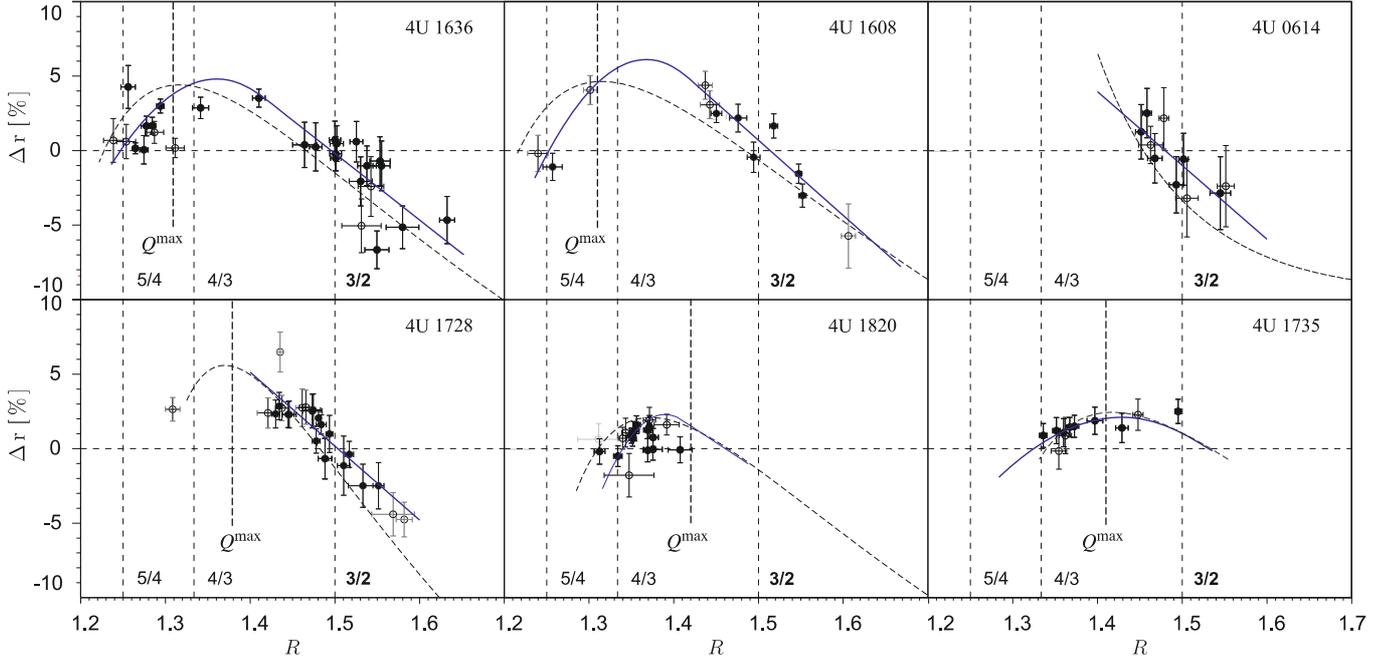
Fig. 2. The dependence of the amplitude difference on the frequency ratio, with detailed view shown of the range $R = 1.2-1.7$. The dashed black curves correspond to Set I (with exponential interpolation), while the individual points correspond to Set II. When there are asymmetric errors, we always use the larger one. The open points are above the 2.5σ threshold; the filled points have significance greater than 3σ. The solid blue curves use linear interpolation in the decreasing part of curve joined to an exponential in the increasing part (see text). The vertical lines labelled with Q^{max} denote the frequency ratio corresponding to the maximum of the lower QPO quality factor (see Sect. 4 for a comment on this).

Table 1. The roots R_1, R_2 of the function $\Delta r(R)$.

Source	Set I				Set II		
	χ_L^2/d.o.f.	χ_U^2/d.o.f.	$R_1(\Delta r = 0)^\dagger$	$R_2(\Delta r = 0)$	χ^2/d.o.f.	$R_1(\Delta r = 0)$	$R_2(\Delta r = 0)$
4U 1608-52	17/38	15/9	1.48 ± 0.01	–	13/8*	1.51 ± 0.01	1.25 ± 0.01
4U 1636-53	1.7/11	40/23	1.49 ± 0.01	–	18/15*	1.49 ± 0.01	1.25 ± 0.01
4U 0614+09	59/15	16/4	1.45 ± 0.01	–	3.8/10*	1.48 ± 0.01	–
4U 1728-34	40/36	6.3/7	1.48 ± 0.01	–	21/23*	1.50 ± 0.01	–
4U 1820-30	23/35	15/7	1.46 ± 0.01	1.31 ± 0.02	32/15	–	1.34 ± 0.02
4U 1735-44	2.6/4	2.5/2	1.53 ± 0.02	1.34 ± 0.01	4.1/8	–	1.33 ± 0.01

† The errors shown correspond to a unit variation of χ^2; for asymmetric errors, we use the larger one; * corresponds to the linear part of curve between $R = 1.4-1.6$.

Fig. 2, more investigation is needed in order to make more precise statements about these two roots. In 4U 1608-52 there are only three relevant datapoints, while in 4U 1636-53 the datapoints give a rather high χ^2 for the increasing part of Δr curve.

For 4U 1820-30 and 4U 1735-44, there is a lack of twin kHz QPO detections around $R \sim 1.5$ from Set II, and we were not able to determine their roots R_1, although the Set I data indicate that they should exist. For the increasing part of the Δr curve, we use the same fitting procedure as for 4U 1608-52 and 4U 1636-53, but we only *expect* the existence of the linear decaying part between $R = 1.4-1.6$, which we determined from the Set I data. In this way, we find the two roots R_2 close to 1.33. For 4U 1820-30, the datapoints close to R_2 are scattered around the R-axis, giving a rather poor χ^2 for all of the fits, and the value of R_2 varies with small changes of χ^2. For 4U 1735-44, the location of R_2 seems to be well-determined.

We note that for 4U 1820-30 and 4U 1735-44 ($R_2 \sim 1.33$), as well as for 4U 1608-52 and 4U 1636-53 ($R_2 \sim 1.25$), the termination of the available data nearly seems to coincide with the position of R_2, which makes the exact determination of R_2 difficult.

4. Discussion and conclusions

In five of the six atoll sources that we have considered (4U 1728−34, 4U 1608−52, 4U 1636−53, 4U 0614+09, and 4U 1820−30), the upper kHz QPO dominates the lower one for high values of the twin kHz QPO ratio ($R > 1.5$) corresponding to low QPO frequencies. The issue of the upper QPO dominance at low QPO frequencies in 4U 1735−44 remains an open question due to the lack of the relevant datapoints in both Sets I and II. The four sources 4U 1728−34, 4U 1608−52, 4U 1636−53, and 4U 0614+09 clearly exhibit the R_1 root close to $R = 1.5$. Because of the lack of datapoints in Set II, however, more investigation is needed to fully confirm a similar statement about R_1 for the sources 4U 1820-30 and 4U 1735-44. For ratios decreasing from the value $R \simeq 1.5$, the difference between the QPO amplitudes reaches its maximum within a narrow interval of $R \in [1.3, 1.45]$[3]. After this,

---

[3] Barret et al. (2005a,b, 2006) determined the frequencies corresponding to maxima of the lower QPO quality factor in the discussed sources. Interestingly, the relevant ratios are close or coincide with those related to the maxima of Δr (see Fig. 2).

as the ratio decreases further (but not for 4U 0614+09 where the available data terminates), the lower QPO starts to lose its dominance again. Notably, all of the determined values of the root R_1 lie inside the ~3% interval around $R = 1.5$, which corresponds to less than 10% of the range $R \in (1.2, 2.5)$. For the four sources (4U 1608-52, 4U 1636-53, 4U 1820-30, 4U 1735-44), and marginally also for 4U 1728-34, there is evidence for of another root (close to $R = 1.33$ or 1.25) where the available data terminate. Most of datapoints in Fig. 2 appear close to the roots R_1 or / and R_2. We therefore suggest that there could be a link between the previously reported ratio clustering and the existence of $R_{1,2}$, which requires further investigation.

Within the framework of the QPO resonance models, the behaviour of the amplitude difference may indicate an energy interchange between the lower and upper QPO modes, typical of non-linear resonances (e.g., Horák & Karas 2006). In this context, it is also rather noticeable that the roots $R_{1,2}$ are *close* to the values 3/2 and 4/3 or 5/4 (which we denoted by dashed vertical lines in the above figures). Nevertheless, in order to take this indication seriously, it is necessary to have a model that gives a detailed explanation of the effect.

Within the scope of the other orbital QPO models, there should also be an explanation for why the roots $R_{1,2}$ appear. For instance, in the case of the relativistic precession model, one can solve equations relating the upper and lower QPO with respect to the radial coordinate ρ, for the particular form of the expressions for the orbital frequencies in Schwarzschild geometry, obtaining the relation $\rho = 6MR^2/(2R - 1)$, see Török et al. (2008). According to this formula, the $R = 1.5$ frequency ratio would correspond to an orbital radius $\rho = 6.75\,M$, which is about 14 km for a neutron star with the "canonical" mass $M = 1.4\,M_\odot$. The 3% scatter around $R = 1.5$ would be projected onto an interval of only about ±1.5% in ρ, i.e., onto ~±0.1 $M \doteq ±200$ m. It is then a question not only of why the observed amplitudes corresponding to oscillations at this radius should be equal, but also why they are equal for several sources at the same radius with a scatter of less than 250 m.

References

Abramowicz, M. A., & Kluźniak, W. 2001, A&A, 374, L19
Abramowicz, M. A., Karas, V., Kluzniak, W., Lee, W. H., & Rebusco, P. 2003, PASJ, 55, 466
Abramowicz, M. A., Barret, D., Bursa, M., et al. 2005a, Astron. Notes, 326, 864
Abramowicz, M. A., Barret, D., Bursa, M., et al. 2005b, in Proceedings of RAGtime 6/7: Workshops on black holes and neutron stars, Opava, 16−18/18−20 September 2004/2005, ed. S. Hledík, & Z. Stuchlík, Opava, Silesian University in Opava, 1
Abramowicz, M. A., Blaes, O. M., Horák, J., Kluzniak, W., & Rebusco, P. 2006, Classical and Quantum Gravity, 23, 5, 1689
Barret, D., Olive, J.-F., & Miller, M. C. 2005a, MNRAS, 361, 855
Barret, D., Olive, J.-F., & Miller, M. C. 2005b, Astronomical Notes, 326, 9, 808
Barret, D., Olive, J., & Miller, M. C. 2006, MNRAS, 370, 1140
Belloni, T., Psaltis, D., & van der Klis, M. 2002, ApJ, 572, 392
Belloni, T., Méndez, M., & Homan, J. 2005, A&A, 437, 209
Belloni, T., Méndez, M., & Homan, J. 2007, MNRAS, 379, 1, 247
Boirin, L., Barret, D., Olive, J., Bloser, P. F., & Grindlay, J. E. 2000
Bradt, H. V., Rothschild, R. E., & Swank, J. H. 1993, A&AS, 97, 355
Bursa, M. 2006, Ph.D. Thesis, Astronomical Institute, Charles University in Prague
Di Salvo, T., Méndez, M., & van der Klis, M. 2003, A&A, 406, 177
Fogelström, S., Levin, L., & Slapak, R. 2008, PASJ, 60, 3
Horák, J., & Karas, V. 2006, A&A, 451, 377
Jahoda, K., Swank, J. H., Giles, A. B., et al. 1996, EUV, X-ray, and Gamma-ray Instrumentation for Astronomy VII, Proc. SPIE, 2808, 59
Jonker, P. G., Méndez, M., & van der Klis, M. 2002, MNRAS, 336, L1
van der Klis, M. 2000, ARA&A, 38, 717
van der Klis, M. 2006, in Compact Stellar X-Ray Sources, ed. W. H. G. Lewin, & M. van der Klis (Cambridge: Cambridge University Press), 39; see also [arXiv:astro-ph/0410551]
Kluźniak, W., & Abramowicz, M. A. 2001, Phys. Rev. Lett., submitted [arXiv:astro-ph/0105057], see also W. Kluźniak, M. A. Abramowicz, 2001, Acta Phys. Pol. B, 32, 3605 [http://th-www.if.uj.edu.pl/acta/vol32/t11.htm]
Lamb, F. K., & Boutloukos, S. 2007, in Short-Period Binary Stars: Observations, Analyses, and Results, ed. E. F. Milone, D. A. Leahy, & D. Hobill (Dordrecht: Springer), Astrophys. Space Sci. Libr., 352
Markwardt, C. B., Strohmayer, T. E., & Swank, J. H. 1999, ApJ, 512, L125
McClintock, J. E., & Remillard, R. A. 2003 [arXiv:astro-ph/0306213]
Méndez, M. 2006, MNRAS, 371, 1925
Méndez, M., & van der Klis, M. 1999, ApJ, 517, L51
Méndez, M., van der Klis, M., Wijnands, R., et al. 1998a, ApJ, 505, L23
Méndez, M., van der Klis, M., & van Paradijs, J. 1998b, ApJ, 506, L117
Méndez, M., van der Klis, M., van Paradijs, J., Lewin, W. H. G., & Vaughan, B. A. 1998c, ApJ, 494, L65
Méndez, M., van der Klis, M., Wijnands, R., Ford, E. C., & van Paradijs, J. 1999, ApJ, 511, L49
Méndez, M., van der Klis, M., & Ford, E. C. 2001, ApJ, 561, 1016
Migliari, S., van der Klis, M., & Fender, R. 2003, MNRAS, 345, L35
Olive, J., Barret, D., & Gierlinski, M. 2003, ApJ, 583, 416
Psaltis, D., Mendez, M., Wijnands, R., et al. 1998, ApJ, 501, L95
Psaltis, D., Wijnands, R., Homan, J., et al. 1999a, ApJ, 520, 763
Psaltis, D., Belloni, T., & van der Klis, M. 1999b, ApJ, 520, 262
Rebusco, P. 2004, PASJ, 56, 553
van Straaten, S., Ford, E. C., van der Klis, M., Méndez, M., & Kaaret, P. 2000, ApJ, 540, 1049
van Straaten, S., van der Klis, M., Di Salvo, T., & Belloni, T. 2002, ApJ, 568, 912
van Straaten, S., van der Klis, M., & Méndez, M. 2003, ApJ, 596, 1155
Stella, L., & Vietri, M. 1999, Phys. Rev. Lett., 82, 17
Török, G., Bakala, P., Stuchlík, Z., & Čech, P. 2008, Acta Astron., 58/1, 1
Zhang, C. M., Yin, H. X., Zhao, Y. H., Zhang, F., & Song, L. M. 2006, MNRAS, 366, 1373